

A Measure of Control for Secondary Cytokine-Induced Injury of Articular Cartilage: A Computational Study

Jason M. Graham¹

October 20, 2017

¹ Department of Mathematics, University of Scranton, Scranton, PA, USA

Abstract

In previous works, the author and collaborators establish a mathematical model for injury response in articular cartilage. In this paper we use mathematical software and computational techniques, applied to an existing model to explore in more detail how the behavior of cartilage cells is influenced by several of, what are believed to be, the most significant mechanisms underlying cartilage injury response at the cellular level. We introduce a control parameter, the radius of attenuation, and present some new simulations that shed light on how inflammation associated with cartilage injuries impacts the metabolic

activity of cartilage cells. The details presented in the work can help to elucidate targets for more effective therapies in the preventative treatment of post-traumatic osteoarthritis.

Keywords: chondrocytes, cytokines, articular cartilage, inflammation

1 Background

Injury response and wound healing is a topic of central importance in biomedical research for obvious reasons. As a result, there has been a great deal of activity in developing mathematical and computational models of wound healing in various organ systems such as skin, see e.g. [12]. In contrast, there has been very little activity in developing computational models for wound healing and injury response in articular cartilage, despite a great interest in this topic in orthopaedics research. What is more, few if any of the mathematical models developed for wound healing in other systems are appropriate for application to articular cartilage.

Articular cartilage is made up of differentiated mesenchymal cells known as chondrocytes. These cells are embedded in an extracellular matrix and are responsible for the biomechanical properties of cartilage [16]. Mechanical stress and injury influence changes in the metabolic activity of chondrocytes [16]. Specifically, during injury response chondrocytes produce and respond to certain cytokines, or signaling molecules, known as tumor necrosis factor α (TNF- α) and erythropoietin (EPO). There is a “balancing act” between

the pro-inflammatory cytokine $\text{TNF-}\alpha$ and the anti-inflammatory cytokine EPO in which each limits the production and biological action of the other. In a recent article Brines and Cerami [3] suggest that $\text{TNF-}\alpha$ plays a significant role in causing the spread of cartilage lesions, while EPO plays an antagonistic role to $\text{TNF-}\alpha$, limiting the area over which a lesion can spread by counteracting some of the effects of inflammation [3]. It has also been observed that there are inherent time-delays in the activation of, and signaling by EPO that results in a window of opportunity for the spread of lesions due to secondary injury caused by inflammation. However, the authors of [3] suggest that it may be possible to intervene with EPO derived therapies to minimize the amount of secondary injury due to inflammation and the spread of cartilage damage.

In previous works [5, 6], the author, with collaborators, develop a novel mathematical model for articular cartilage injury response aiming to test hypotheses put forth in [3]. As with any mathematical or computational model, it is important to understand how the behavior of the results depend on the parameter values. In particular, it is useful to know how changes in the parameter values effect the results of simulations. This is especially the case when the goal is to tie the modeling efforts to experimental results. On the one hand, any measurement involves an error and if the model is sensitive to small changes in the parameter values, often the case when models contain nonlinear terms, the experimental error may be significant enough that simulations behave differently than what is to be expected, based on experimental

observations. On the other hand, different parameter values may correspond to different types of observed behavior, or even more interestingly, changes in parameter values can lead to predictions about the system being modeled. One of the goals of the models described in [5, 6] is to understand the balance between pro-inflammatory cytokines such as TNF- α and anti-inflammatory cytokines such as EPO. We can use the mathematical models together with computational techniques to help understand this balance by exploring how changes in parameters related to different aspects of TNF- α and EPO dynamics simulate different types of behavior in cartilage injury response. This paper is devoted to such an exploration. In particular, we would like to know how changes in parameter values corresponding to different properties of the TNF- α /EPO interactions influence the lesion expansion or abatement properties during cartilage injury response.

The remainder of this paper is organized as follows. The next section provides a brief description of a mathematical model, described fully in [5, 6]¹, to which, in this paper, we apply computational methods to explore some issues regarding the behavior of chondrocytes during the typical injury response in articular cartilage. It is in that section where we establish ideas and notation that is used throughout the remainder of this work. The third section, the results section, shows the computational results and discusses

¹We note that there is a slight difference between the models in [5], and in [6]. In this work we use the model in [5] as it gives the same (qualitative) results but replaces a discontinuous term with a continuous term, and also replaces a phenomenological parameter with one that is more directly connected to the biology.

their significance. The paper ends with conclusions drawn from the results section.

2 Materials and Methods

Here we briefly summarize the mathematical model, established in [5, 6], used to obtain the computational results of the next section. During injury, chondrocytes are considered as being in specific and distinct “states” corresponding to which cytokines the cells are capable of producing and responding to. We refer to the normal state of a subpopulation of chondrocytes as the healthy state. As a result of inflammation and injury, healthy chondrocytes can enter into a “sick” class in which they are at risk of undergoing programmed cell death. The sick cells are considered as being in one of two states:

1. the catabolic state
2. the EPOR active state

Cells in the catabolic state are characterized by their ability to produce TNF- α , while EPOR active cells are characterized by their ability to express a receptor for EPO. We note that these two cell states are distinct in that cells capable of producing TNF- α are not capable of expressing the EPO receptor, and vice versa. Another consequence of cells being in the catabolic state is that they produce reactive oxygen species (ROS) which serves as a

catalyst for the production of EPO by cells in the healthy state.

Due to the fact that there are two typical means of cell death: necrosis, and programmed cell death known as apoptosis, we also consider two states for the “dead” class of subpopulations of chondrocytes. We note that for the purposes considered herein, apoptotic cells do not feed back into the system. Due to the abrupt nature of the injury, we assume that the initial injury results in necrosis of cells at the injury site. Furthermore, we assume that cell death due to secondary cytokine-induced injury is strictly through apoptosis. The reasoning here is that necrosis is a nonspecific event that occurs in cases of severe pathological cell and tissue damage, whereas secondary cytokine-induced injury corresponds with a physiologic form of cell death used to remove cells in a more orderly and regulated fashion and there is evidence that often, this is via apoptosis [4].

The typical injury response can be summarized as follows. An injury results in cell necrosis and the release of alarmins (such as damage-associated molecular pattern molecules DAMPs), which initiate the chemical cascade associated with the innate immune and cartilage injury responses [2, 7]. The DAMPs signal healthy cells near the injury to enter the catabolic state, catabolic cells are capable of the production of $\text{TNF-}\alpha$ which is fundamental to inflammation. The inflammatory cytokine $\text{TNF-}\alpha$ has multifold effects on the system: It

1. feeds back to promote further switching of cells in the healthy state into cells in the catabolic state,

2. causes cells in the catabolic state to enter the EPOR active state, in which they express a receptor for EPO and are no longer capable of synthesizing TNF- α [3],
3. influences apoptosis of cells in the catabolic and EPOR active states,
4. degrades extracellular matrix (denoted by U) which results in increased concentrations of DAMPs,
5. has a limiting effect on production of EPO [3].

Catabolic cells also produce reactive oxygen species (ROS) which influences the production of EPO by healthy cells. We denote the concentration of ROS at a given time and location by R . There is a time delay of 20–24 hours before a healthy cell signaled by ROS will begin to produce EPO [3].

In the following we use the notation, as in [5, 6], for the mathematical model of chondrocyte/cytokine interactions during injury response:

1. R - concentration of reactive oxygen species (ROS) at a given time and spatial location
2. M - concentration of alarmins (DAMPs) at a given time and spatial location
3. F - concentration of the pro-inflammatory cytokine TNF- α at a given time and spatial location

4. P - concentration of the anti-inflammatory cytokine EPO at a given time and spatial location
5. U - density of extra-cellular matrix at a given time and spatial location
6. C - population density of healthy cells at a given time and spatial location
7. S_T - population density of catabolic cells at a given time and spatial location
8. S_A - population density of EPO receptor (EPOR) active cells at a given time and spatial location
9. D_N - population density of necrotic cells at a given time and spatial location

The equations making up the mathematical model developed in [5, 6] are

$$\partial_t R = \nabla \cdot (D_R \nabla R) - \delta_R R + \sigma_R S_T, \quad (1a)$$

$$\partial_t M = \nabla \cdot (D_M \nabla M) - \delta_M M + \sigma_M D_N + \delta_U U \frac{F}{L_F + F}, \quad (1b)$$

$$\partial_t F = \nabla \cdot (D_F \nabla F) - \delta_F F + \sigma_F S_T, \quad (1c)$$

$$\partial_t P = \nabla \cdot (D_P \nabla P) - \delta_P P + \sigma_P C(t - \tau_2) \frac{R(t - \tau_2)}{L_R + R(t - \tau_2)} \frac{K_F}{K_F + F}, \quad (1d)$$

$$\begin{aligned} \partial_t C = & \alpha S_A \frac{P}{L_P + P} - \beta_1 C \frac{M}{L_M + M} \frac{K_P}{K_P + P} \\ & - \beta_2 C \frac{F}{L_F + F} \frac{K_P}{K_P + P}, \end{aligned} \quad (1e)$$

$$\begin{aligned} \partial_t S_T = & \beta_1 C \frac{M}{L_M + M} \frac{K_P}{K_P + P} + \beta_2 C \frac{F}{L_F + F} \frac{K_P}{K_P + P} \\ & - \gamma S_T(t - \tau_1) \frac{F(t - \tau_1)}{L_F + F(t - \tau_1)} - \nu S_T \frac{F}{L_F + F} \frac{M}{L_M + M}, \end{aligned} \quad (1f)$$

$$\begin{aligned} \partial_t S_A = & \gamma S_T(t - \tau_1) \frac{F(t - \tau_1)}{L_F + F(t - \tau_1)} - \alpha S_A \frac{P}{L_P + P} \\ & - \mu_{S_A} S_A \frac{F}{L_F + F}, \end{aligned} \quad (1g)$$

$$\partial_t D_N = -\eta D_N, \quad (1h)$$

$$\partial_t U = -\delta_U U \frac{F}{L_F + F}. \quad (1i)$$

Table 1 describes the meaning and units of the model parameters. The baseline parameter values for the model appear in table 1 of [6]. By baseline we mean values that are either taken from the literature, or fit to give quantitative or qualitative agreement with biological observations.

Parameter	Meaning	Units
D_R	Diffusion Coefficient	$\frac{\text{cm}^2}{\text{day}}$
D_M	Diffusion Coefficient	$\frac{\text{cm}^2}{\text{day}}$
D_F	Diffusion Coefficient	$\frac{\text{cm}^2}{\text{day}}$
D_P	Diffusion Coefficient	$\frac{\text{cm}^2}{\text{day}}$
δ_R	Natural Decay Rate	$\frac{1}{\text{day}}$
δ_M	Natural Decay Rate	$\frac{1}{\text{day}}$
δ_F	Natural Decay Rate	$\frac{1}{\text{day}}$
δ_P	Natural Decay Rate	$\frac{1}{\text{day}}$
δ_U	Rate of Degradation of ECM by TNF- α	$\frac{1}{\text{day}}$
σ_R	Production Rate	$\frac{\text{micromolar}\cdot\text{cm}^2}{\text{day}\cdot\text{cells}}$
σ_M	Production Rate	$\frac{\text{micromolar}\cdot\text{cm}^2}{\text{day}\cdot\text{cells}}$
σ_F	Production Rate	$\frac{\text{micromolar}\cdot\text{cm}^2}{\text{day}\cdot\text{cells}}$
σ_P	Production Rate	$\frac{\text{micromolar}\cdot\text{cm}^2}{\text{day}\cdot\text{cells}}$
K_F	Rate limiting concentration for TNF- α	micromolar
K_P	Rate limiting concentration for EPO	micromolar
L_R	Saturation constant for ROS	micromolar
L_M	Saturation constant for DAMPs	micromolar
L_F	Saturation constant for TNF- α	micromolar
L_P	Saturation constant for EPO	micromolar
α	Response rate of EPOR active cells to EPO	$\frac{1}{\text{day}}$
β_1	Response rate of healthy cells to DAMPS/EPO	$\frac{1}{\text{day}}$
β_2	Response rate of healthy cells to TNF- α /EPO	$\frac{1}{\text{day}}$
γ	Response rate of catabolic cells to TNF- α	$\frac{1}{\text{day}}$
η	Rate of degradation of necrotic cells	$\frac{1}{\text{day}}$
ν	Response rate of catabolic cells to TNF- α /DAMPs	$\frac{1}{\text{day}}$
μ_{S_A}	Response rate of EPOR active cells to TNF- α	$\frac{1}{\text{day}}$
τ_1	time delay in catabolic response	days
τ_2	time delay in production of EPO	days

Table 1: Description and units of the parameters appearing in the model (1a)-(1i).

In order to compare the simulation results with *in vitro* observations it is useful to choose a “measurable”, i.e. a quantity, that can be derived from results using the model, and easily measured from experiment. Here we consider the **radius of attenuation**, this is defined to be the smallest radius beyond which a lesion cannot expand due to the actions of EPO. In the computational simulations, it is observed that the radius of attenuation varies with the change in parameter values. In the following, we will compute the radius of attenuation as certain specific parameters are varied. To remain consistent with experiment, we consider injuries to a piece of circular cartilage of diameter 2.5cm and a time frame of about ten days. In each of the results discussed below we choose a pair of parameters, then use the mathematical model to compute how the radius of attenuation varies, as the given pair of parameters is varied in a systematic way.

How the radius of attenuation varies as dependent on a given pair of parameters tells us the influence of those parameters on the lesion expansion, or abatement during cartilage injury response. Based on this information we gain insight into which aspects of the chondrocyte/cytokine interactions are most relevant to target in potential therapies. This is one of the principal motivations for the development of the mathematical model in the first place. Furthermore, when one parameter in the given pair corresponds to a TNF- α related term and the other the associated EPO term, we gain insight into the details of the TNF- α /EPO balancing act discussed in [3].

3 Results and Discussion

For all of the following simulations, as in [5, 6], we choose the spatial domain to be a circle of radius 2.5 cm. This is biologically reasonable since articular cartilage is divided into three zones [16], with the zone forming the surface of cartilage, the superficial zone, containing the highest cell density [16]. Furthermore, we assume circular symmetry, since the diffusion of the cytokines tend to be in the radial direction. This allows for the system (1) to be reduced to a problem in one spatial dimension. We choose initial conditions to represent an initial injury occurring at the center of the domain covering a disc of radius 0.25 cm. This is typical of the types of impact experiments that are often performed in orthopaedics labs. The boundary conditions are taken to be no-flux, i.e.

$$\left. \frac{\partial W}{\partial r} \right|_{r=2.5} = 0 \quad (2)$$

for $W = R, M, F, P, C, S_T, S_A, D_N, U$. This essentially states that the cytokines are confined domain, and are only removed through natural decay processes. We note that since the system (1) contains delay terms we must specify not only a condition at time $t = 0$ but also a history for some time interval $(-T, 0)$. For time values less than zero, the time of the initial injury, we take the history to correspond to no injury, i.e. the total cell population is in the healthy state.

To carry out numerical approximations of the system (1) we discretize in

space as follows. Consider the diffusion equation with circular symmetry in conservative, or divergence, form

$$\frac{\partial u(r, t)}{\partial t} = \nabla_r \cdot J := \frac{1}{r} \frac{\partial}{\partial r} (rJ), \quad (3)$$

where $J = D \frac{\partial u}{\partial r}$ is the flux, and D is the diffusion coefficient. Partition the radii as $r_i, i = 0, \dots, n$ by dividing the circle into concentric annuli. Then for $0 < i < n$ we discretize (3) by the formula

$$\pi \left(r_{i+\frac{1}{2}}^2 - r_{i-\frac{1}{2}}^2 \right) \frac{\partial u(r_i, t)}{\partial t} = 2\pi r_{i+\frac{1}{2}} J_{i+\frac{1}{2}} - 2\pi r_{i-\frac{1}{2}} J_{i-\frac{1}{2}}, \quad (4)$$

where $J_{i\pm\frac{1}{2}}$ is the flux at $r_{i\pm\frac{1}{2}} := \frac{r_i + r_{i\pm 1}}{2}$, given explicitly by

$$J_{i+\frac{1}{2}} = \frac{u_{i+1} - u_i}{r_{i+\frac{1}{2}} - r_{i-\frac{1}{2}}}, \quad (5)$$

$$J_{i-\frac{1}{2}} = \frac{u_i - u_{i-1}}{r_{i+\frac{1}{2}} - r_{i-\frac{1}{2}}}. \quad (6)$$

This leads to

$$\frac{\partial u(r_i, t)}{\partial t} = \Delta_i := \frac{r_{i+\frac{1}{2}} J_{i+\frac{1}{2}} - r_{i-\frac{1}{2}} J_{i-\frac{1}{2}}}{\frac{1}{2} \left(r_{i+\frac{1}{2}}^2 - r_{i-\frac{1}{2}}^2 \right)}. \quad (7)$$

We observe that

$$\frac{1}{2} \left(r_{i+\frac{1}{2}}^2 - r_{i-\frac{1}{2}}^2 \right) = \frac{1}{2} (r_{i+\frac{1}{2}} + r_{i-\frac{1}{2}}) (r_{i+\frac{1}{2}} - r_{i-\frac{1}{2}}) \quad (8)$$

$$= r_i \delta r_i, \quad (9)$$

where $r_i = \frac{r_{i+\frac{1}{2}} + r_{i-\frac{1}{2}}}{2}$, and $\delta r_i = r_{i+\frac{1}{2}} - r_{i-\frac{1}{2}}$. Thus, the scheme (7) corresponds to the standard finite difference approximation in polar coordinates, see for example [13].

For the case $i = 0$, that is, at the center of the circle, we have

$$\pi r_{\frac{1}{2}}^2 \frac{\partial u(0, t)}{\partial t} = 2\pi r_{\frac{1}{2}} J_{\frac{1}{2}}, \quad (10)$$

which gives

$$\frac{\partial u(0, t)}{\partial t} = \Delta_0 := \frac{J_{\frac{1}{2}}}{\frac{1}{2} r_{\frac{1}{2}}}. \quad (11)$$

Finally, for a no-flux boundary condition as in (2), the differencing is given by

$$\pi (r_n^2 - r_{n-\frac{1}{2}}^2) \frac{\partial u(r_n, t)}{\partial t} = -2\pi r_{n-\frac{1}{2}} J_{n-\frac{1}{2}}, \quad (12)$$

which gives

$$\frac{\partial u(r_n, t)}{\partial t} = \Delta_n := \frac{-r_{n-\frac{1}{2}} J_{n-\frac{1}{2}}}{\frac{1}{2} (r_n^2 - r_{n-\frac{1}{2}}^2)}. \quad (13)$$

These formulas are reproduced from appendix C of [1]²

Applying (7), (11), and (13) to the spatial terms in (1a),(1b),(1c), and (1d) then gives a semi-discrete system of delay-differential equations

$$\partial_t R_i = \Delta_i - \delta_R R_i + \sigma_R (S_T)_i, \quad (14a)$$

$$\partial_t M_i = \Delta_i - \delta_M M_i + \sigma_M (D_N)_i + \delta_U U_i \frac{F_i}{L_F + F_i}, \quad (14b)$$

$$\partial_t F_i = \Delta_i - \delta_F F_i + \sigma_F (S_T)_i, \quad (14c)$$

$$\partial_t P_i = \Delta_i - \delta_P P_i + \sigma_P C_i(t - \tau_2) \frac{R_i(t - \tau_2)}{L_R + R_i(t - \tau_2)} \frac{K_F}{K_F + F_i}, \quad (14d)$$

$$\begin{aligned} \partial_t C_i = & \alpha(S_A)_i \frac{P_i}{L_P + P_i} - \beta_1 C_i \frac{M_i}{L_M + M_i} \frac{K_P}{K_P + P_i} \\ & - \beta_2 C_i \frac{F_i}{L_F + F_i} \frac{K_P}{K_P + P_i}, \end{aligned} \quad (14e)$$

$$\begin{aligned} \partial_t (S_T)_i = & \beta_1 C_i \frac{M_i}{L_M + M_i} \frac{K_P}{K_P + P_i} + \beta_2 C_i \frac{F_i}{L_F + F_i} \frac{K_P}{K_P + P_i} \\ & - \gamma(S_T)_i(t - \tau_1) \frac{F_i(t - \tau_1)}{L_F + F_i(t - \tau_1)} - \nu(S_T)_i \frac{F_i}{L_F + F_i} \frac{M_i}{L_M + M_i}, \end{aligned} \quad (14f)$$

$$\begin{aligned} \partial_t (S_A)_i = & \gamma(S_T)_i(t - \tau_1) \frac{F_i(t - \tau_1)}{L_F + F_i(t - \tau_1)} - \alpha(S_A)_i \frac{P_i}{L_P + P_i} \\ & - \mu_{S_A}(S_A)_i \frac{F_i}{L_F + F_i}, \end{aligned} \quad (14g)$$

$$\partial_t (D_N)_i = -\eta(D_N)_i, \quad (14h)$$

$$\partial_t U_i = -\delta_U U_i \frac{F_i}{L_F + F_i}, \quad (14i)$$

for $i = 0, \dots, n$, where Δ_i is the appropriate discrete circularly symmetric

²We note that in [1] there are misprints in the formulas corresponding to (12), (13) which have here been corrected.

diffusion operator from (7),(11), or (13). The semi-discrete system is solved in MATLAB using the delay-differential equation solver `dde23`. For details on the methods and software for solving delay-differential equations see [9, 10, 11].

The primary parameter pairs of interest are the time delays τ_1, τ_2 , the diffusion coefficients D_F, D_P for TNF- α and EPO respectively, the production rates σ_F, σ_P for TNF- α and EPO respectively, and the saturation constants K_F, K_P for TNF- α and EPO respectively. These are the parameters that are most closely tied to the balancing act between pro- and anti-inflammatory cytokines, and this is what is of primary interest to researchers working to develop therapies to minimize the collateral damage associated with inflammation in cartilage injuries.

The first pair of parameters we vary are the time delay parameters τ_1, τ_2 . We recall that τ_1 is the delay that for catabolic cells signaled by TNF- α to become EPOR active, while τ_2 is the delay for a healthy cell signaled by reactive oxygen species (ROS) to synthesize EPO. The baseline values for the delays are 12 hours for τ_1 and 24 hours for τ_2 [3, 6]. Figure 1 shows the radius of attenuation as it varies with τ_1, τ_2 over the domain $[0, 10] \times [0, 10]$ with units in days. We observe that the delay parameter τ_2 has a more significant impact on the radius on attenuation than does τ_1 . Since τ_2 corresponds to the delay in a healthy cell signaled by reactive oxygen species to produce EPO, our results support the hypothesis in [3] that intervention with exogenous EPO is an important step in limiting the amount of collateral damage caused by

TNF- α .

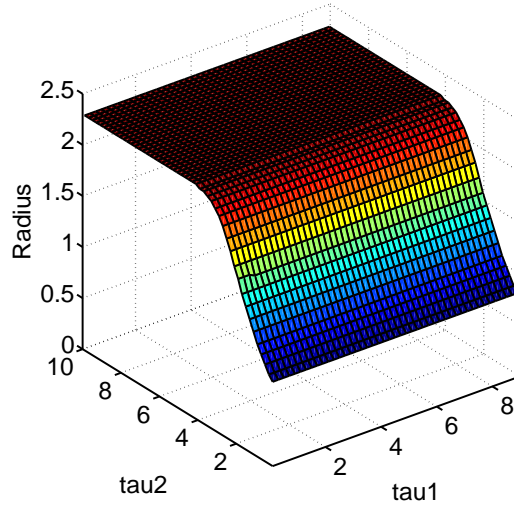


Figure 1: Radius of attenuation as it varies simultaneously with τ_1, τ_2 , with other parameters held fixed.

Now we consider the effects of varying the diffusion coefficients D_F, D_P for TNF- α and EPO respectively. We note that the diffusion of cytokines is the principal mechanism that determines the spatial behavior of lesion spreading in articular cartilage. The baseline values for D_F, D_P are 0.05, $0.005 \frac{\text{mm}^2}{\text{day}}$ respectively [6, 8]. Figure 2 shows the radius of attenuation as a function of D_F, D_P over the domain $[0, 0.1] \times [0, 0.015]$. We observe that, of the two diffusion parameters, D_F has the greater impact on the radius of attenuation. This is somewhat expected in light of the fact that there is a time delay for production of EPO by healthy cells signaled by ROS. Because of this delay TNF- α is typically produced at significantly earlier times than

EPO. Thus the degree to which TNF- α can diffuse significantly influences how far the lesion can spread during this initial time period before there are sufficient concentrations of EPO to abate the spread of damage.

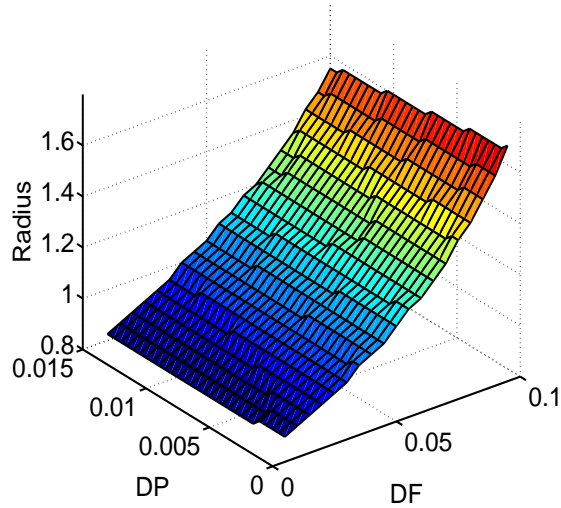


Figure 2: Radius of attenuation as it varies simultaneously with D_F, D_P , with other parameters held fixed.

Next, we consider the radius of attenuation as it varies simultaneously with the saturation constants K_F and K_P . The baseline values for these parameters are 10 and 1 respectively, with units in micromoles. Figure 3 shows the radius of attenuation as a function of K_F, K_P over the domain $[0, 100] \times [0, 100]$ with units in micromoles. This is quite a large variation for K_F and K_P . We observe that the saturation constant, K_P , for EPO to limit the response of healthy cells to TNF- α and alarmins (DAMPs) has the greater influence of the two parameters K_F, K_P on the radius of attenuation.

Thus the results of the mathematical model seem to suggest that healthy cells must be sensitive to relatively low concentrations of EPO in order to minimize damage, and for maximal healing to occur. Figure 4 again shows the radius of attenuation as a function of K_F, K_P but for a smaller range in the parameter values. Here we focus on values relatively close to the baseline values, this gives an idea of how sensitive the model is to small, simultaneous changes in values for the parameters K_F, K_P . The results are consistent with those shown in figure 3.

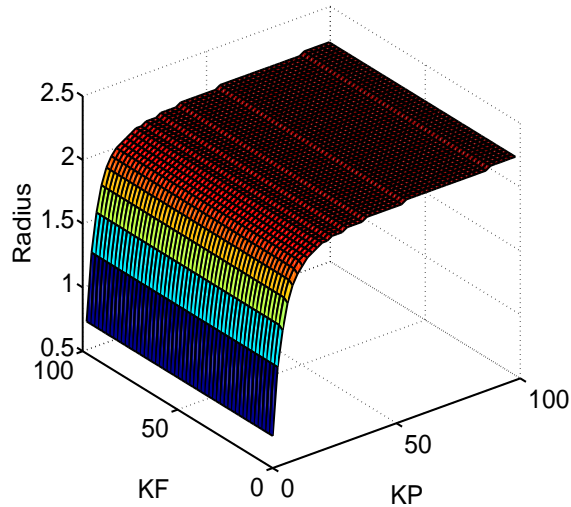


Figure 3: Radius of attenuation as it varies simultaneously with K_F, K_P , with other parameters held fixed.

We observed that when comparing the saturation parameters K_F, K_P , the parameter K_P has the more significant effect on the radius of attenuation. However, the term involving K_P and TNF- α in the model system (1a)-(1i)

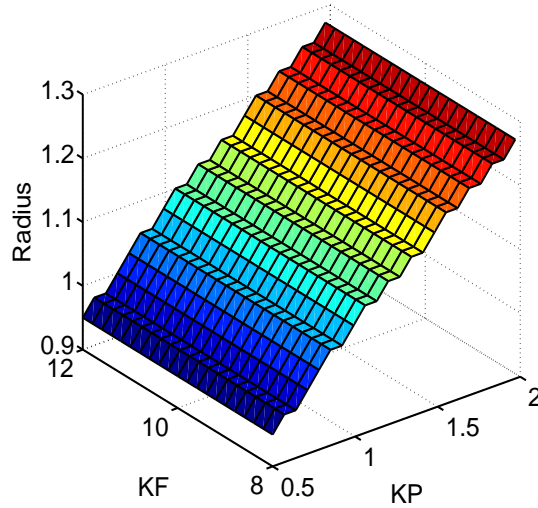


Figure 4: Radius of attenuation as it varies simultaneously with K_F, K_P , with other parameters held fixed.

is

$$\beta_2 C \frac{F}{L_F + F} \frac{K_P}{K_P + P}, \quad (15)$$

which influences the switch from the healthy to the catabolic state. Thus, the switching is determined by the parameters β_2 and K_P together. We examine the radius of attenuation as a function of β_2, K_P , the results are shown in figure 5. Again it is observed that K_P has the more significant impact in determining the radius of attenuation.

We next examine the radius of attenuation as it varies simultaneously with the production rates σ_F, σ_P of TNf- α and EPO respectively. The baseline values for these parameters are 0.0001 for σ_F and 0.001 for σ_P with units in days⁻¹. Figure 6 shows the radius of attenuation as a function of σ_F, σ_P

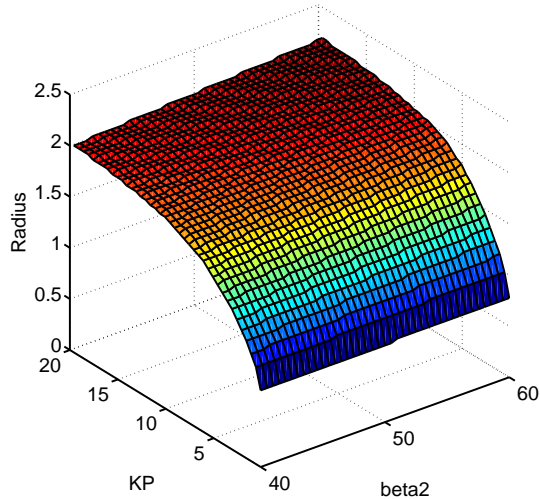


Figure 5: Radius of attenuation as it varies simultaneously with β_2, K_P , with other parameters held.

over the domain $[0, 0.0001] \times [0, 0.1]$. We observe that, overall, the radius of attenuation increases as σ_F , the production of TNF- α , increases. However, the radius of attenuation appears to be a nonlinear function of σ_F, σ_P . In figure 7 we show the radius of attenuation as a function of σ_F, σ_P over the domain $[0, 0.0003] \times [0.001, 0.005]$. This shows that, while the radius of attenuation is generally increasing as a function of σ_F , that for a fixed value of σ_P there is a point beyond which the radius of attenuation exceeds the domain. Thus, for our domain, if σ_F is sufficiently large then there is no radius of attenuation. However, this does not necessarily imply that no healing whatsoever can take place.

Figure 8 shows the dynamics of the healthy and penumbral (sum of

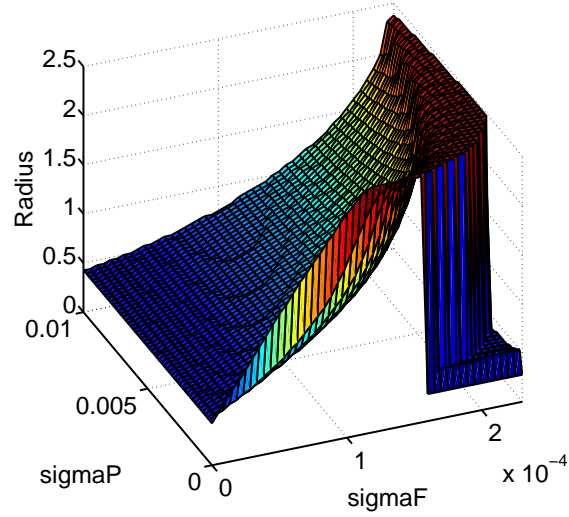


Figure 6: Radius of attenuation as it varies simultaneously with σ_F, σ_P , with other parameters held.

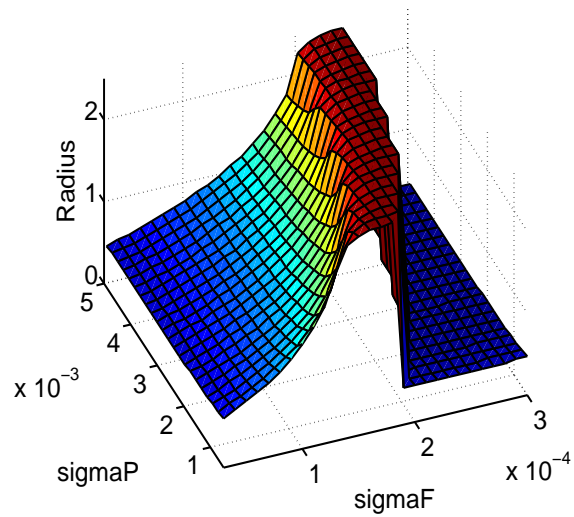


Figure 7: Radius of attenuation as it varies simultaneously with σ_F, σ_P , with other parameters held fixed.

catabolic and EPOR active) cell populations for values of σ_F and σ_P that, according to figure 7, lead to a radius of attenuation of approximately 1.7cm. Since the radius of attenuation in figure 7 is computed based on a ten day time period, figure 8(i) shows the cell populations as a function of radius after a twenty day period to ensure that the radius does not continue to expand after ten days. We observe that, while the radius of attenuation is larger than that in figure 6 of [6], there is still at least as much healing near the initial injury site due to EPOR active cells switching back to healthy as a result of EPO signaling. An interesting observation is the “dip” in the healthy cell population between radius $r = 0.25cm$ and $r = 0.7$ if figure 8(d). This is due to the fact that diffusion of TNF- α results in lower concentrations of TNF- α for smaller radius values where there is a higher concentration of EPOR active cells. Thus, the EPOR active cells can more effectively response to EPO.

Figure 9 shows the dynamics of the healthy and penumbral (sum of catabolic and EPOR active) cell populations for values of σ_F and σ_P that, according to figure 7, lead to no radius of attenuation, that is, there is no point in our domain for which secondary TNF- α induced damage cannot spread. Again, we point out that this does not imply that no healing occurs. We see in figure 9(i) that after twenty days there is a significant healthy cell population despite that the penumbra spread throughout the entire domain. We again see in figure 9(i) the “dip” in the healthy population which is now more pronounced than in figure 8(d).

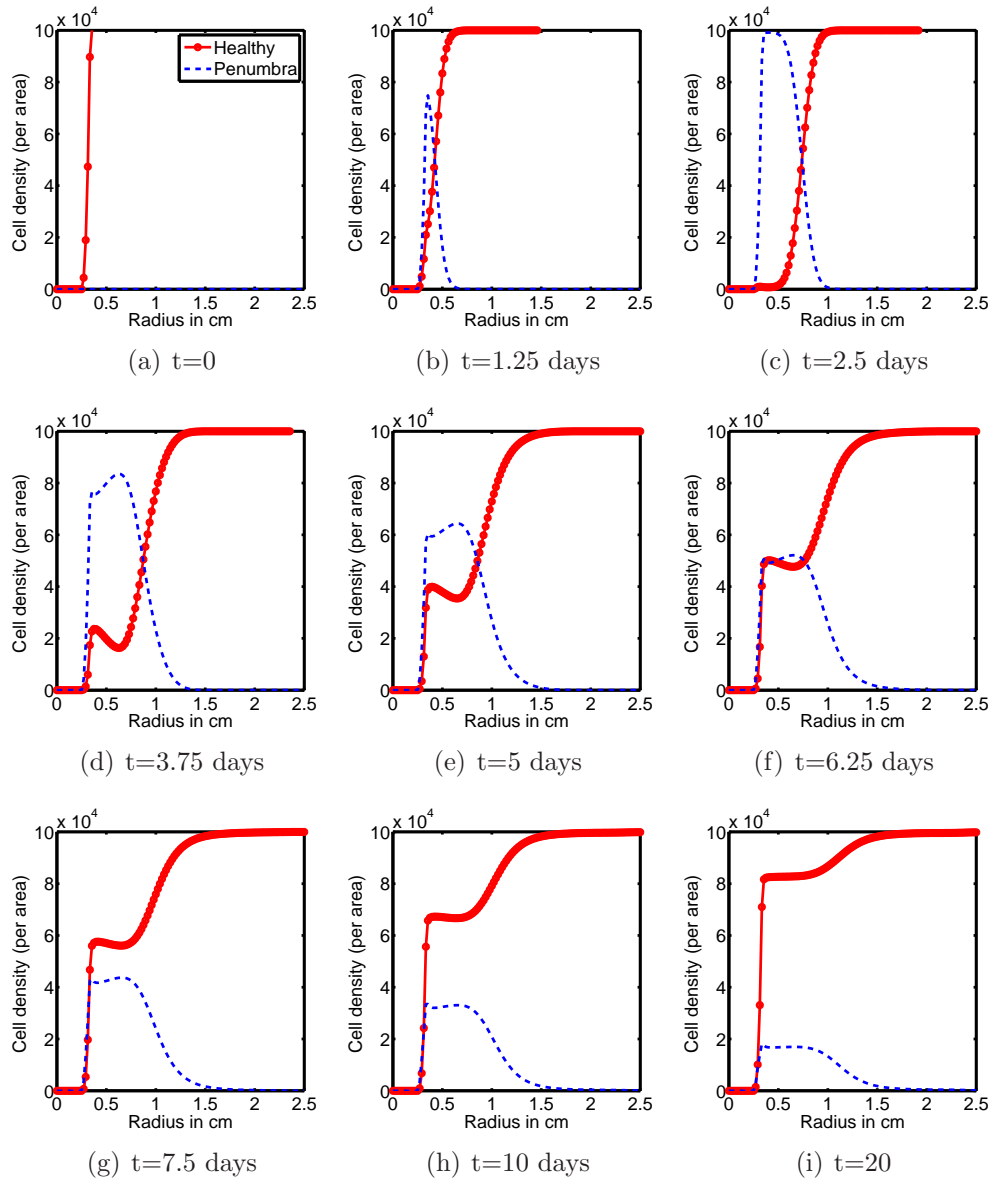


Figure 8: Cell populations when $\sigma_F = 0.00017$ and $\sigma_P = 0.0032$.

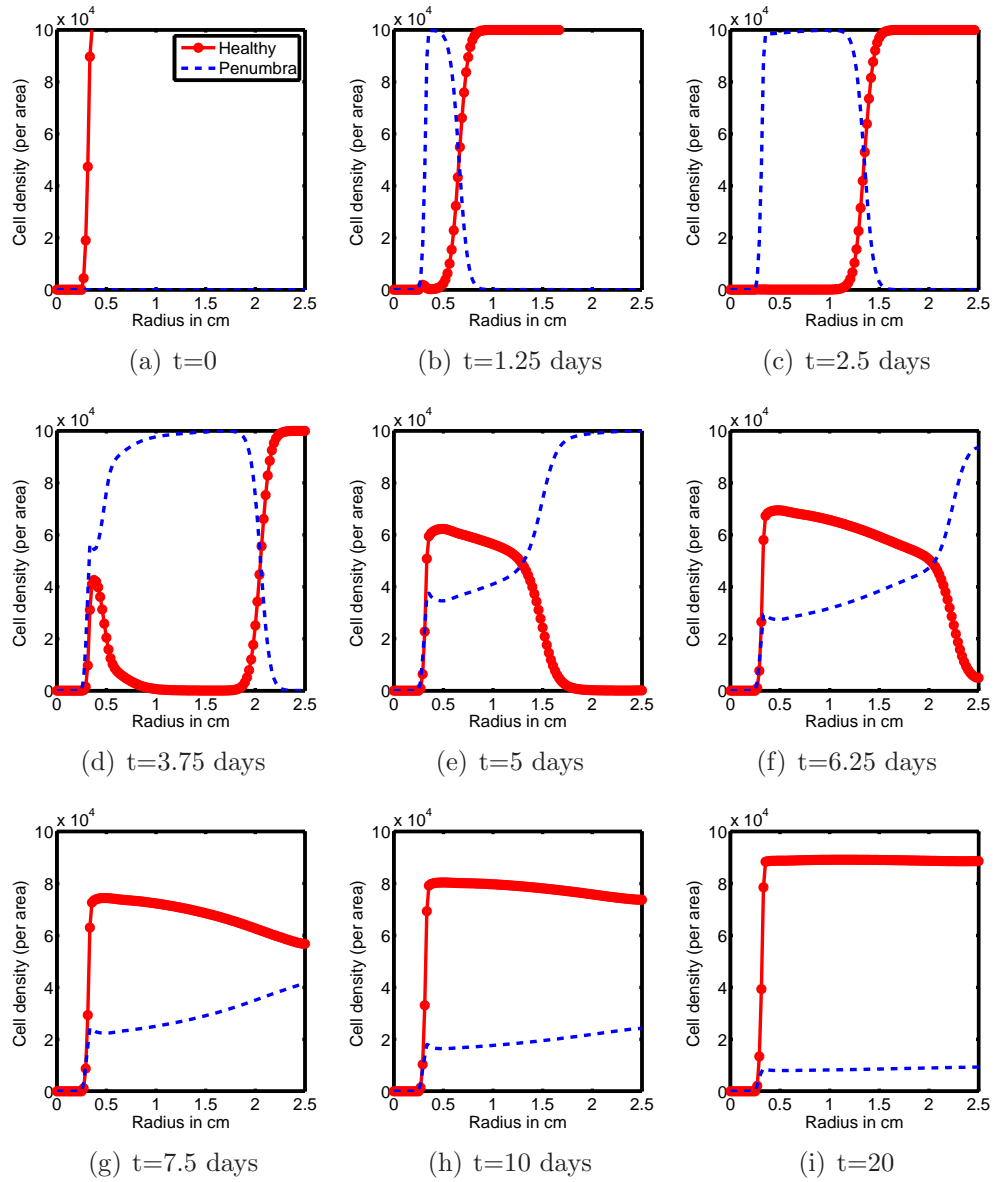


Figure 9: Cell populations when $\sigma_F = 0.0004$ and $\sigma_P = 0.003$.

We make one further observation. If the production rate σ_F of TNF- α is set to zero, according to the equations in system (1a)-(1i) there should be a penumbra made up entirely of catabolic cells. Figure 10 shows the cell population density profile for healthy and catabolic cells after ten days. We see that it is indeed the case that there is a penumbra made up entirely of catabolic cells. This result suggests that a delay in the production of TNF- α could allow for the build up of a large population of catabolic cells, so that, once TNF- α is produced there will be a wave of apoptosis and EPOR activation. Depending on the concentration of EPO available this scenario could lead to more damage than is typical. Thus, damage associated with a delay in the production of TNF- α could potentially be worse in some cases than is seen with just the delay in the production of EPO.

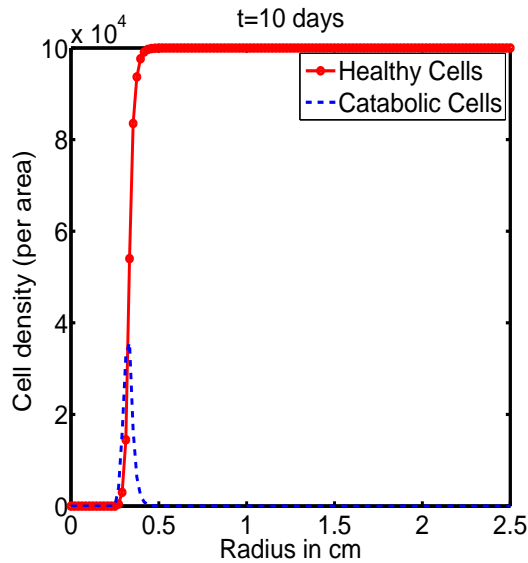


Figure 10: Cell populations after 10 days with $\sigma_F = 0$.

4 Conclusions

The work in the previous section is an incomplete exploration of parameter space. We note however that it does suggest that the ratio $\frac{\sigma_P}{\sigma_F}$ between the EPO production rate and the TNF- α production rate plays a significant role in determining the radius of attenuation. The results shown in figures 8, and 9 imply that EPO, or more generally the anti-inflammatory arm of cartilage injury response is robust. Even in cases where the ratio $\frac{\sigma_P}{\sigma_F}$ is small but nonzero inflammation does not result in the uncontrolled spread of injury as in the case when $\sigma_P = 0$. It is ultimately desirable to derive theoretical results that give complete detailed knowledge of the qualitative behavior of solutions to system (1a)-(1i) as a function of the parameter values. This is a difficult problem due to the number of equations and large number of parameter values. One future direction for the work presented above is its application to real experiments. It is common in orthopaedics research to perform impact experiments on large animal joints, typically bovine or porcine, or harvested human joints in attempts to replicate cell-level pathology in intra-articular fractures, see *e.g.* [15, 14]. It is likely that cytokine measurements relevant to the work presented here can be made from such experimental studies. Another future direction for the work presented here and in [5, 6] is to include mechanical effects that are important in cartilage injury. Of particular interest is the representation of effects associated with shear stress to cartilage. In general, articular cartilage in joints such as the knees and ankles can respond

efficiently to direct impact mechanical stress. However, cartilage is less resistant to shear stress. A mathematical and computational models that are capable of giving insight into what happens when shear stress is applied will be of great value to orthopaedics research.

5 Acknowledgements

The author would like to thank Bruce Ayati, Jim Martin, Prem Ramakrishnan, and Lei Ding for valuable discussions regarding this work. The author would like to express sincere gratitude to the editor and reviewers for their valuable comments and suggestions.

References

- [1] B.P. Ayati. *Methods for computational population dynamics*. ProQuest LLC, Ann Arbor, MI, 1998. Thesis (Ph.D.)—The University of Chicago.
- [2] M. E. Bianchi. Damps, pamps and alarmins: all we need to know about danger. *J. Leukoc. Biol.*, 81:1–5, 2006.
- [3] M. Brines and A. Cerami. Erythropoietin-mediated tissue protection: reducing collateral damage from the primary injury response. *J. Intern. Med.*, 264:405–432, 2008.

- [4] M. Del Carlo and R.F. Loeser. Cell death in osteoarthritis. *Current rheumatology reports*, 10(1):37–42, 2008.
- [5] J.M. Graham. *Mathematical representations in musculoskeletal physiology and cell motility*. ProQuest LLC, Ann Arbor, MI, 2012. Thesis (Ph.D.)–The University of Iowa.
- [6] J.M. Graham, B.P. Ayati, L. Ding, P.S. Ramakrishnan, and J.A. Martin. Reaction-diffusion-delay model for epo/tnf- α interaction in articular cartilage lesion abatement. *Biology Direct*, 7(9), 2012.
- [7] H. E. Harris and A. Raucchi. Alarming news about danger. *EMBO Reports*, 7(8):774–778, 2006.
- [8] H.A. Leddy and F. Guilak. Site-specific molecular diffusion in articular cartilage measured using fluorescence recovery after photobleaching. *Annals of Biomedical Engineering*, 31(7):753–760, 2003.
- [9] L. F. Shampine and M. W. Reichelt. The matlab ode suite. *SIAM J. Sci. Comput.*, 18(1):1–22, 1997.
- [10] L. F. Shampine and S. Thompson. Solving ddes in matlab. *Appl. Numer. Math.*, 37(4):441–458, 2001.
- [11] L. F. Shampine and S. Thompson. *Numerical solution of delay differential equations*. Springer, New York, 2009.

- [12] J.A. Sherratt and J.D. Murray. Models of epidermal wound healing. *Proc. Bio. Sci.*, 241(1300):29–36, 1990.
- [13] J. W. Thomas. *Numerical partial differential equations: finite difference methods*, volume 22 of *Texts in Applied Mathematics*. Springer-Verlag, New York, 1995.
- [14] Y. Tochigi, P. Zhang, M.J. Rudert, T.E. Baer, J.A. Martin, S.L. Hillis, and T.D. Brown. A novel impaction technique to create experimental articular fractures in large animal joints. *Osteoarthritis and Cartilage*, 21(1):200 – 208, 2013.
- [15] Yuki Tochigi, Joseph A. Buckwalter, James A. Martin, Stephen L. Hillis, Peng Zhang, Tanawat Vaseenon, Abigail D. Lehman, and Thomas D. Brown. Distribution and progression of chondrocyte damage in a whole-organ model of human ankle intra-articular fracture. *The Journal of Bone & Joint Surgery*, 93(6):533–539, 2011.
- [16] M. Ulrich-Vinther, M.D. Maloney, Schwarz E.M., Rosier R., and R.J. O’Keefe. Articular cartilage biology. *J. Am. Acad. Orthop. Surg.*, 11(6):421–430, 2003.

